Immune Netw. 2022 Apr;22(2):e14
https://doi.org/10.4110/in.2022.22.e14
pISSN 1598-2629·eISSN 2092-6685

IMMUNE NETWORK

Original Article

Mitochondrial Transplantation Ameliorates the Development and Progression of Osteoarthritis

A Ram Lee[1,2,†], Jin Seok Woo[1,†], Seon-Yeong Lee[1,†], Hyun Sik Na[1,2], Keun-Hyung Cho[1,2], Yeon Su Lee[1,2], Jeong Su Lee[1,2], Seon Ae Kim[3], Sung-Hwan Park[1,4], Seok Jung Kim[3,*], Mi-La Cho[1,2,5,*]

[1]Rheumatism Research Center, College of Medicine, Catholic Research Institute of Medical Science, The Catholic University of Korea, Seoul 06591, Korea
[2]Department of Biomedicine & Health Sciences, College of Medicine, The Catholic University of Korea, Seoul 06591, Korea
[3]Department of Orthopedic Surgery, College of Medicine, The Catholic University of Korea, Seoul 06591, Korea
[4]Division of Rheumatology, Department of Internal Medicine, Seoul St. Mary's Hospital, College of Medicine, The Catholic University of Korea, Seoul 06591, Korea
[5]Department of Medical Lifescience, College of Medicine, The Catholic University of Korea, Seoul 06591, Korea

Received: Aug 18, 2021
Revised: Dec 23, 2021
Accepted: Dec 27, 2021
Published online: Jan 21, 2022

***Correspondence to**
Seok Jung Kim
Department of Orthopedic Surgery, College of Medicine, The Catholic University of Korea, 222 Banpo-daero, Seocho-gu, Seoul 06591, Korea.
Email: peter@catholic.ac.kr

Mi-La Cho
Rheumatism Research Center, College of Medicine, Catholic Research Institute of Medical Science, The Catholic University of Korea, 222 Banpo-daero, Seocho-gu, Seoul 06591, Korea.
Email: iammila@catholic.ac.kr

†These authors contributed equally to this work.

ORCID iDs
Jin Seok Woo
https://orcid.org/0000-0001-8921-2832
Mi-La Cho
https://orcid.org/0000-0001-5715-3989

Conflict of Interest
The authors declare no potential conflicts of interest.

ABSTRACT

Osteoarthritis (OA) is a common degenerative joint disease characterized by breakdown of joint cartilage. Mitochondrial dysfunction of the chondrocyte is a risk factor for OA progression. We examined the therapeutic potential of mitochondrial transplantation for OA. Mitochondria were injected into the knee joint of monosodium iodoacetate-induced OA rats. Chondrocytes from OA rats or patients with OA were cultured to examine mitochondrial function in cellular pathophysiology. Pain, cartilage destruction, and bone loss were improved in mitochondrial transplanted-OA rats. The transcript levels of IL-1β, TNF-α, matrix metallopeptidase 13, and MCP-1 in cartilage were markedly decreased by mitochondrial transplantation. Mitochondrial function, as indicated by membrane potential and oxygen consumption rate, in chondrocytes from OA rats was improved by mitochondrial transplantation. Likewise, the mitochondrial function of chondrocytes from OA patients was improved by coculture with mitochondria. Furthermore, inflammatory cell death was significantly decreased by coculture with mitochondria. Mitochondrial transplantation ameliorated OA progression, which is caused by mitochondrial dysfunction. These results suggest the therapeutic potential of mitochondrial transplantation for OA.

Keywords: Osteoarthritis; Mitochondrial dysfunction; Mitochondrial transplantation; Autophagy; Necroptosis

INTRODUCTION

Osteoarthritis (OA) is a common degenerative joint disease that results from breakdown of joint cartilage and underlying bone. OA is characterized by the infiltration of immune cells into cartilage and cartilage destruction (1,2). The risk factors for OA include joint injury, age, obesity, and gender, and it causes pain, stiffness, bone spurs, and swelling (3,4). Although

IMMUNE NETWORK

Abbreviations

BCA, bicinchoninic acid; CT, computed tomography; LAMP1, lysosomal-associated membrane protein 1; MLKL, mixed lineage kinase domain-like protein; MMP-13, matrix metallopeptidase 13; MIA, monosodium iodoacetate; MTDR, MitoTracker Deep Red; OA, osteoarthritis; pMLKL, phospho mixed lineage kinase domain-like protein; pRIP1, phospho receptor-interacting protein 1; PWL, paw withdrawal latency; PWT, paw withdrawal threshold; RIPK1, receptor-interacting protein kinase 1; STIM1, stromal interaction molecule 1; TEM, transmission electron microscope.

Author Contributions

Conceptualization: Lee AR, Woo JS, Lee SY, Cho ML; Formal analysis: Lee AR, Na HS, Cho KH; Investigation: Lee AR, Cho ML; Methodology, Lee AR, Na HS, Cho KH, Lee YS, Lee JS, Kim SA; Software: Lee AR, Woo JS, Lee SY; Validation: Lee AR, Woo JS, Lee SY, Cho ML; Writing - original draft:: Lee AR, Woo JS; Writing - review & editing: Park SH, Kim SJ, Cho ML.

OA does not affect life expectancy, it significantly disrupts the quality of life. Drug treatment is focused on pain relief, not on the progression of OA.

Mitochondria are complex and dynamic organelles, whose main function is energy production for the maintenance of cellular homeostasis (5,6). The number of mitochondria depends on cell type, and they typically occupy ≤20% of the cell volume (7). Chondrocytes are the only cell type in healthy cartilage (8). Recent studies have reported mitochondrial dysfunction, including mitochondrial respiratory chain enzyme complex activities and membrane potential, in chondrocytes of OA patients (9). Mitochondrial dysfunction leads to cartilage degeneration by suppressing ATP production, depolarizing the mitochondrial membrane, increasing oxidative stress, disrupting calcium homeostasis, and altering mitochondrial DNA (10-13). Mitochondrial dysfunction has been reported in OA chondrocytes, inducing an imbalance between anabolism and catabolism of extracellular matrix (14,15) and decreasing mitochondrial complex activity (16,17).

Autophagy is a self-degradative cellular and molecular mechanism that removes dysfunctional or unnecessary proteins and organelles (18). The OA environment increases ROS levels, impeding autophagolysosome progression via mitochondrial and lysosomal dysfunction (19). Accumulation of autophagosomes caused by lysosomal dysfunction promotes OA progression and activation of lysosomal function by metformin ameliorates OA progression (20).

Mitochondrial transplantation has been proposed to be a novel therapeutic intervention for heart injury, kidney injury, neurodegenerative diseases, and cancer (21-25). Mitochondrial transplantation enhances ATP synthesis, oxygen consumption, and cell viability, thereby improving systemic function. Also, mitochondrial transplantation has immunomodulatory effects in the sepsis mouse model (26).

Based on the above, mitochondrial transplantation is being investigated as a therapeutic target for many diseases, but not in OA. We examined the therapeutic potential of mitochondrial transplantation for OA and observed that mitochondrial transplantation ameliorates OA progression. Inflammatory cell death and autophagy were improved by mitochondrial transplantation. Our findings demonstrate for the first time the therapeutic potential of mitochondrial transplantation for OA.

MATERIALS AND METHODS

Induction of OA in rat

Male Wistar rats (180–250 g, 7 wk of age) were purchased from Central Lab Animal Inc. (Seoul, Korea). Animals were randomly assigned to the treatment or control group before the study began. After anesthetization with isoflurane, 7-week-old male Wistar rats (n=5) were injected with 3 mg of monosodium iodoacetate (MIA; I2512, Sigma, St. Louis, MO, USA), dissolved in a 50 μL of saline, using a 26.5 G needle inserted through the patellar ligament into the intra-articular space of the right knee. Mitochondria were administered to 10 μg/50 μL volume twice weekly in the right knee intra-articular space of MIA-induced rats, and rats in the control group were injected with the same volume of saline.

https://doi.org/10.4110/in.2022.22.e14

Isolation of mitochondria from L6 cells and human muscle

Mitochondria were isolated from L6 rat cells using a Mitochondrial Isolation Kit for Cultured Cells (89874; Thermo, Waltham, MA, USA). Briefly, 3×10^6 L6 cells were incubated with 400 μL of reagent A for 2 min on ice with vortexing every minute and incubated with 5 μL of reagent B for 5 min on ice. After adding 400 μL of reagent C, cells were centrifuged at 700 × g for 10 min at 4°C. The supernatant was transferred to a new tube and centrifuged at 12,000 × g for 15 min at 4°C. The pellet (mitochondria) was washed with 400 μL of reagent C and centrifuged at 12,000 × g for 5 min at 4°C. Mitochondria from muscle tissue of OA patients were isolated according to Boutagy et al. (27). Protein concentrations were quantified by bicinchoninic acid (BCA) assay (23235; Thermo).

Rat and human articular chondrocyte differentiation and culture

Isolation of chondrocytes was performed as described previously (20). Briefly, chondrocytes were isolated from the cartilage of MIA-induced OA rats and patients. Cartilage was digested with 0.5 mg/mL hyaluronidase, 5 mg/mL protease type XIV, and 2 mg/mL collagenase type V. Chondrocytes were incubated DMEM with 10% fetal bovine serum. Rat chondrocytes of passage 1 were cultured and analyzed. Human chondrocytes were cultured in the presence or absence of IL-1β (20 ng/mL) or TNF-α (50 mg/ml), and 5 μg of isolated mitochondria for 24 h.

Assessment of pain behavior

Nociception in MIA-treated rats was tested using a dynamic plantar aesthesiometer (Ugo Basile, Gemonio, Italy). The device is an automated version of the von Frey hair assessment procedure and is used to assess mechanical sensitivity. When the instrument was activated, a fine plastic monofilament advanced at a constant speed and touched the paw in the proximal metatarsal region. The filament exerted a gradually increasing force on the plantar surface, starting below the threshold of detection and increasing until the stimulus became painful, as indicated by the rat's withdrawal of its paw. The force required to elicit a paw-withdrawal reflex was recorded automatically and measured in g. A maximum force of 50 g and a ramp speed of 25 s were used for all aesthesiometer tests. Weight balance in MIA-treated rats was analyzed using an incapacitance meter (IITC Life Science, Woodland Hills, CA, USA). The rats were allowed to acclimate for 5 min in an acrylic holder. After 5 min, both feet of the rat were fixed to the pad and the weight balance was measured for 5 s. Three measurements were repeated in the same manner. The weight of the unguided and guided legs was determined and substituted in the formula to calculate the percentage. The percentage value was calculating by comparing the legs with and without OA.

Histopathological analysis

Knee joints were collected from each group 3 wk after MIA induction. The tissues were fixed in 10% formalin after decalcification using Decalcifying Solution-Lite (Sigma), and embedded in paraffin. Tissue was stained with H&E and safranin O and analyzed by the Osteoarthritis Research Society International and the Mankin scoring system (28).

Immunohistochemistry

Paraffin-embedded sections were incubated at 4°C with the following primary monoclonal antibodies: anti-IL-1β (ab9722; Abcam, Cambridge, UK), anti-TNF-α (ab6671; Abcam), anti-matrix metallopeptidase 13 (MMP-13; ab39012; Abcam), anti-MCP-1 (ab7202; Abcam) and anti-phospho-mixed lineage kinase domain-like protein (ab196436; Abcam). The samples were next incubated with the respective secondary biotinylated Abs, followed by incubation for 30 min with streptavidin–peroxidase complex. The reaction product was developed using 3,3-diaminobenzidine chromogen (K3468, Dako; Agilent, Santa Clara, CA, USA).

In vivo micro-computed tomography

Micro-computed tomography (CT) was performed using a bench-top cone-beam type *in vivo* animal scanner (mCT 35; SCANCO Medical, Wangen-Brüttisellen, Switzerland). The animals were imaged at settings of 70 kVp and 141 μA using a 0.5-mm-thick aluminum filter. The pixel size was 8.0 μm and the rotation step was 0.4°. Cross-sectional images were reconstructed using a filtered back-projection algorithm (NRecon software, Bruker micro CT; Bruker, Kontich, Belgium). For each scan, a stack of 286 cross-sections was reconstructed at 2,000 × 1,335 pixels. Bone volume and surface were analyzed at the femur.

Electron microscopy

Electron microscopy was performed as described previously (29). Briefly, cells were fixed in 4% paraformaldehyde and 2.5% glutaraldehyde in 0.1 M phosphate buffer overnight at 4°C. The cells were washed in 0.1 M phosphate buffer, postfixed with 1% osmium tetroxide for 1 h at 4°C, dehydrated in graded ethyl alcohol solutions, exchanged in acetone, and embedded in Epon 812. Ultrathin sections (70–80 nm) were obtained on an ultramicrotome (Leica Ultracut; Leica, Vienna, Austria) and stained with uranyl acetate and lead citrate. Images were acquired at 60 kV using a transmission electron microscope (TEM, JEM 1010; JEOL, Tokyo, Japan).

CTX-II enzyme-linked immunosorbent assay

CTX-II level from the serum of MIA-induced OA model was performed based on the method of the CTX-II (E-EL-R2554; Elabscience, Houston, TX, USA) kit.

ATP assay

Isolated mitochondrial ATP content was analyzed using the ATP Lite Luminescence Assay System (6016943; Perkin Elmer, Seer Green, UK).

Coculture of osteoarthritic human chondrocytes with mitochondria

OA chondrocytes were seeded in 24-well plates at 5×10^4/well with isolated mitochondria (5 μg) in 10% DMEM. One day later, the cell culture medium was replaced with 0.1% insulin–transferrin–selenium-A–DMEM, and isolated mitochondria were layered onto the OA chondrocytes. Cells were incubated at 37°C for 24 h and harvested for further experiments.

Mitochondrial analysis by flow cytometry

Delivery of exogenous mitochondria to human chondrocytes was confirmed by Mitotracker deep red (MTDR, M22426; Thermo) staining. The mitochondrial membrane potential was measured by JC-1 (T3168; Thermo) staining. The mitochondrial ROS level was measured by MitoSOX (M36008; Thermo) staining, and analyzed by flow cytometry on a FACS Calibur instrument (BD Biosciences, Franklin Lakes, NJ, USA).

Annexin V and propidium-iodide staining

Chondrocytes were harvested and stained with fluorescein isothiocyanate-conjugated Annexin V and propidium iodide (K101-100; BD Biosciences) for 5 min at room temperature. Flow cytometric analysis was performed on a FACS Calibur instrument (BD Biosciences).

Autophagy staining and confocal laser scanning microscopy

OA chondrocytes with isolated mitochondria were cocultured for 1 day. For confocal staining of LC3 and p62, lysosomal-associated membrane protein 1 (LAMP1) cells were plated in four-well chamber slides, washed with PBS, fixed in 4% paraformaldehyde, washed with PBS, and blocked with 10% normal goat serum for 30 min. The cells were stained at 4°C overnight with

anti-LC3 (ab48394; Abcam), anti-LAMP1 (sc-20011; Santa Cruz Biotechnology, Santa Cruz, CA, USA), and anti-p62 (ab56416; Abcam) Abs. The primary Ab was detected using a phycoerythrin-conjugated antirabbit IgG secondary Ab for 2 h at room temperature, and nuclei were stained with DAPI (D3571; Invitrogen, Waltham, MA, USA). Stained cells were analyzed using a confocal microscope (LSM 510 Meta; Zeiss, Oberkochen, Germany). The expression of LC3, p62, and LAMP1 was estimated by comparing the mean fluorescence intensity using LSM 510 Meta.

Western blotting

The protein levels of Ki-67 (nb600-1252; Novus Bio, Littleton, CO, USA), stromal interaction molecule 1 (STIM1, PA5-20371; Invitrogen), COX IV (CST4850; Cell Signaling, Danvers, MA, USA), Tubulin (ab6161; Abcam), LAMP1 (sc-20011; Santa Cruz Biotechnology), p62 (ab56416; Abcam), LC3 (ab48394; Abcam), phospho mixed lineage kinase domain-like protein (pMLKL, ab184718; Abcam), mixed lineage kinase domain-like protein (MLKL, CS214789; EMD Millipore, Danvers, MA, USA), phospho receptor-interacting protein 1 (pRIP1, 65746S; Cell Signaling), RIP1 (PA5-20811; Thermo), pRIP3 (ab209384; Abcam), RIP3 (13526S; Cell Signaling), and GAPDH (ab181602; Abcam) were measured by western blotting (SNAP i.d. Protein Detection System; Merck Millipore, Danvers, MA, USA). Cells were incubated in six-well plates with IL-1β (20 ng/mL) in the presence or absence of mitochondria (5 μg) for 24 h, and mitochondrial and whole-cell lysates were prepared. Protein concentration was measured by BCA assay (23235, Thermo), and samples were separated on a 4%–12% sodium dodecyl sulfate-polyacrylamide gel and transferred to a nitrocellulose membrane (Amersham Pharmacia, Uppsala, Sweden). Primary Abs to Ki-67, STIM1, COX IV, Tubulin, LC3, p62, LAMP1, pMLKL, MLKL, receptor-interacting protein kinase 1 (RIPK1), RIPK3, and GAPDH were diluted in 0.1% skim milk in Tris-buffered saline Tween-20 and incubated for 15 min at room temperature. The membrane was washed and incubated with horseradish peroxidase-conjugated secondary Ab for 10 min at room temperature. Band density was estimated by image-capture densitometry.

Reverse transcription-quantitative real-time PCR

mRNA was extracted using TRIzol (Molecular Research Center, Cincinnati, OH, USA). cDNA was synthesized using the Superscript Reverse Transcription system (Takara, Shiga, Japan), and qPCR was performed using LightCycler FastStart DNA Master SYBR Green I (Takara) following the manufacturer's instructions. Expression values were normalized to that of β-actin. Primer sequences are listed in **Supplementary Table 1**.

Ethics approval and consent of participate

The experimental procedures were reviewed and approved by the Catholic University Animal Care and Ethics Committee (approval No. 2021-0078-01). OA patient were recruited from the Orthopedic Surgery, Uijeongbu St. Mary's Hospital, Seoul, Korea (IRB No. UC21TISI0069).

Statistical analysis

Results are means ± SEM. Data were analyzed by Student's *t*-test or Mann-Whitney *U* test using Prism 5 software (GraphPad, La Jolla, CA, USA). $p<0.05$ (2-tailed) was considered indicative of significance.

RESULTS

Isolation of mitochondria

11.68±0.68 μg of mitochondria were obtained from 1×10^6 of L6 cells (**Fig. 1A**). Contamination during mitochondrial isolation was confirmed by immunoblotting using Ki-67, STIM1, tubulin, and Cox4, which are located in the nuclear, endoplasmic reticulum, cytosol, and inner mitochondrial membrane, respectively (**Fig. 1B**). Flow cytometry for the mitochondrial marker, nonyl acridine orange, showed that the isolated mitochondria showed 96.7% purity (**Fig. 1C**). The ATP content of isolated mitochondria was measured using three different amounts of mitochondria (**Fig. 1D**).

Attenuation of OA progression by mitochondrial transplantation

The clinical phenotypes, including paw withdrawal latency (PWL), the paw withdrawal threshold (PWT), and weight-bearing, were improved in mitochondrial-injected rats compared to the controls (**Fig. 1E and F**). Therefore, mitochondrial injection suppresses the progression of OA by suppressing the pain sensation and severity of the OA model. CTX-II is a degradation product of type II collagen, a component of cartilage, and its serum level is increased in severe OA. The CTX-II level was decreased in the mitochondrial transplanted group (**Fig. 1G**). Histological and micro-CT data showed that destruction of joint and bone loss was improved in the mitochondria-transplanted group. Safranin O staining and micro-CT data showed cartilage destruction and bone loss in the knee joint of the vehicle group, which were improved in the mitochondria-transplantation group (**Fig. 1H and I**). Micro-CT showed that mitochondrial administration reduces bone damage in the knee joint (**Fig. 1J**). Bone surface and bone volume were significantly increased in the mitochondria-transplantation group compared to the vehicle group (**Fig. 1K**).

Downregulation of proinflammatory cytokines in the knee joint of MIA-induced rat

The expression of the proinflammatory cytokines IL-1β, TNF-α, MMP-13 (catabolic factor), and pMLKL (necrosis marker) was decreased in the mitochondria-transplantation group (**Supplementary Fig. 1A and B**). Therefore, mitochondrial transplantation ameliorates OA progression by regulating inflammation.

Improvement of mitochondrial function by mitochondria transfer in rat OA chondrocytes

We observed mitochondrial swelling and cristae structural changes and a decreased number of mitochondria in chondrocytes of the vehicle group compared to the WT (uninduced OA) and these changes were rescued by mitochondrial transplantation (**Fig. 2A and B**). Such changes are typically associated with mitochondrial dysfunction and were rescued by mitochondrial transplantation. Depolarization of mitochondrial membrane was observed in the vehicle group and was rescued in the mitochondria-transplantation group (**Fig. 2C**).

Improvement of mitochondrial function by mitochondria transfer in OA chondrocytes

To confirm the intracellular transmission of mitochondria, isolated mitochondria were stained with MTDR and cocultured with human chondrocytes. MTDR stained mitochondria were transmitted intracellularly at 24 h after coculture with chondrocytes (**Fig. 3A and B**). The expression of the OXPHOS complex was measured in chondrocytes after culture with IL-1β (20 ng/mL) for 24 h in the presence or absence of mitochondria. The expression of

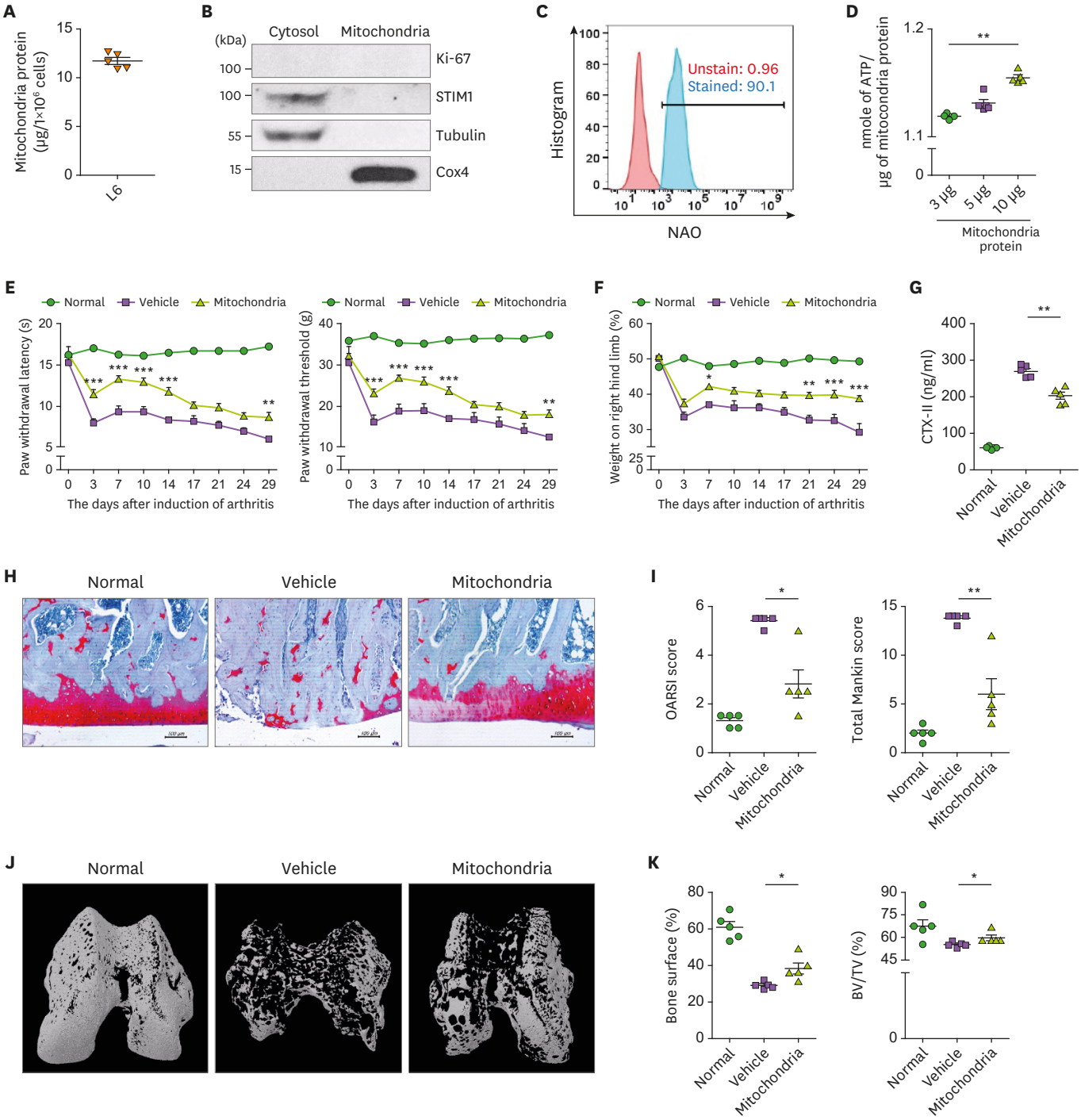

Figure 1. Attenuation of OA by mitochondrial transplantation. (A) Bar graph shows the amount of isolated mitochondria from 1x10^6 of L6 cells. (B) Representative immunoblots show the expression of Ki-67, STIM1, tubulin, and COX4 in the nuclear, ER, cytosolic, and mitochondrial fractions, respectively. (C) Isolated mitochondira stained with NAO. Representative FACS plot shows percentage of NAO positive mitochondria. (D) Bar graph shows average ATP content of isolated mitochondria. MIA-induced OA rats were observed and evaluated for 29 days (n=5 animals per group). The mitochondrial injection was performed intra-articularly twice weekly. Kinetics of PWL, PWT (E), and weight-bearing (F). (G) Bar graph shows the average amount of CTX-II in serum of each group. (H) Representative images of Safranin O-stained cartilage. Scale bar = 100 μm. (I) Average total Mankin score (left) and OARIS score (right). (J) Representative micro CT images of bone. (K) Percentage of bone surface (left) and BV: TV ratio (right). Data are means ± SEM.
NAO, nonyl acridine orange.
*p<0.05, **p<0.01.

https://doi.org/10.4110/in.2022.22.e14

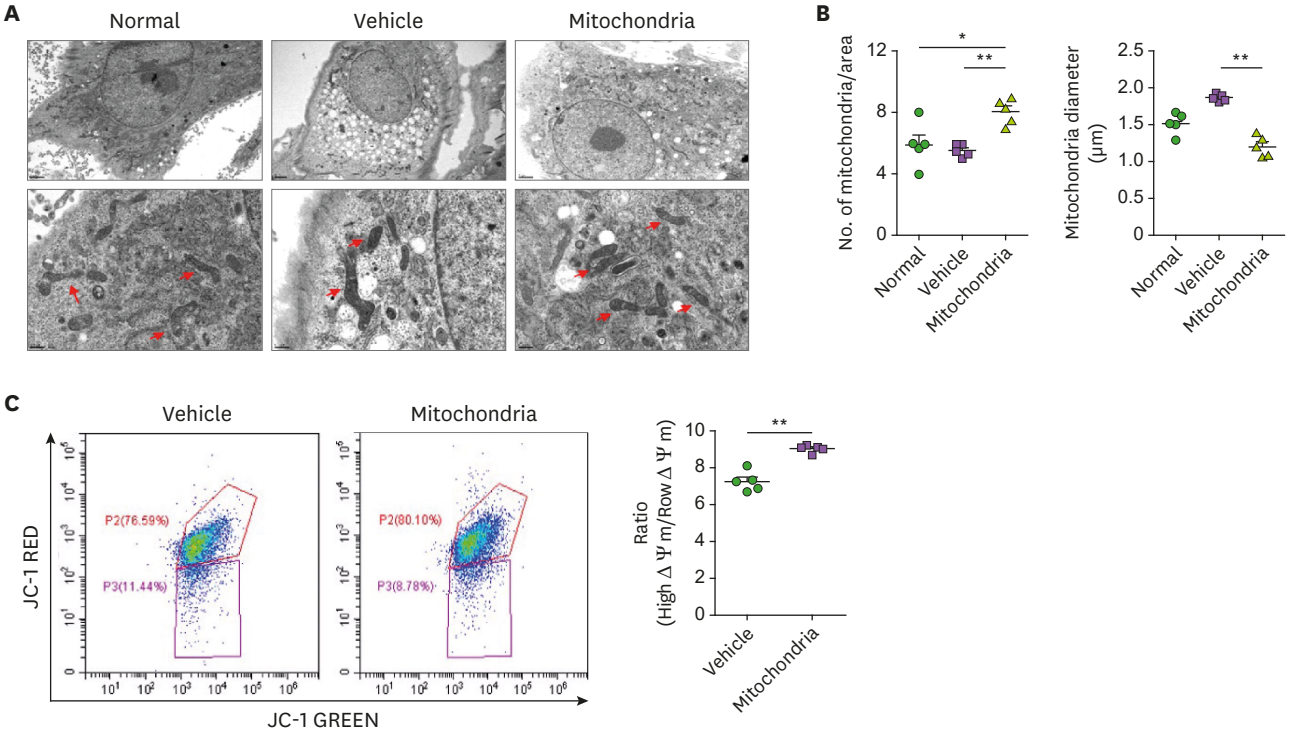

Figure 2. Improvement of mitochondrial function in chondrocytes of OA rats by mitochondrial transplantation. Chondrocytes were isolated from normal, MIA-induced OA rat, and mitochondrial transplanted-MIA-induced OA rats. (A) Representative transmission electron microscopy images show mitochodria in chondrocytes of each group. Red arrow, mitochondria. Scale bar, 2 μm (upper panels) and 0.5 μm (lower panels). (B) Bar graph shows averaged number of mitochondria (left) and mitochondrial diameter (right) in each group. (C) Mitochondrial membrane potential was measured by JC-1 staining. Data are means ± SEM. $^{*}p<0.05$, $^{**}p<0.01$.

complexes IV and V was increased in the mitochondria-transplantation group (**Fig. 3C**) and the mitochondrial membrane potential was significantly increased (**Fig. 3D**). We observed mitochondrial swelling, which was rescued by mitochondria transplantation, as in MIA-induced OA rats (**Fig. 3E and F**).

Regulation of autophagy by mitochondrial transplantation

The increased ROS levels in OA impede autophagolysosome progression by inducing mitochondrial and lysosomal dysfunction (19). The ROS level was increased in OA chondrocytes treated with IL-1β and was decreased in the mitochondria-transplantation group (**Fig. 4A**). The expression of LC-3II (autophagy flux marker) and LAMP1 (lysosome marker) in chondrocytes was significantly increased and decreased, respectively, by IL-1β treatment and was rescued by mitochondrial transplantation (**Fig. 4B**). These results were confirmed by confocal microscopy and TEM. The colocalization between LC3 and P62 (autophagosome) was increased in the presence of IL-1β, however, the colocalization of LC3-LAMP1 (autophagolysosom3) was increased under the condition of mitochondrial transplantation (**Fig. 4C and D**). Also, TEM data showed that autophagosome (red arrow) was decreased in the presence of IL-1β, and autophagolysosome (yellow arrow) was increased under the condition of mitochondrial transplantation (**Fig. 4E and F**). Our data indicate that mitochondrial transplantation improves mitochondrial function through the regulation of autophagy.

https://doi.org/10.4110/in.2022.22.e14

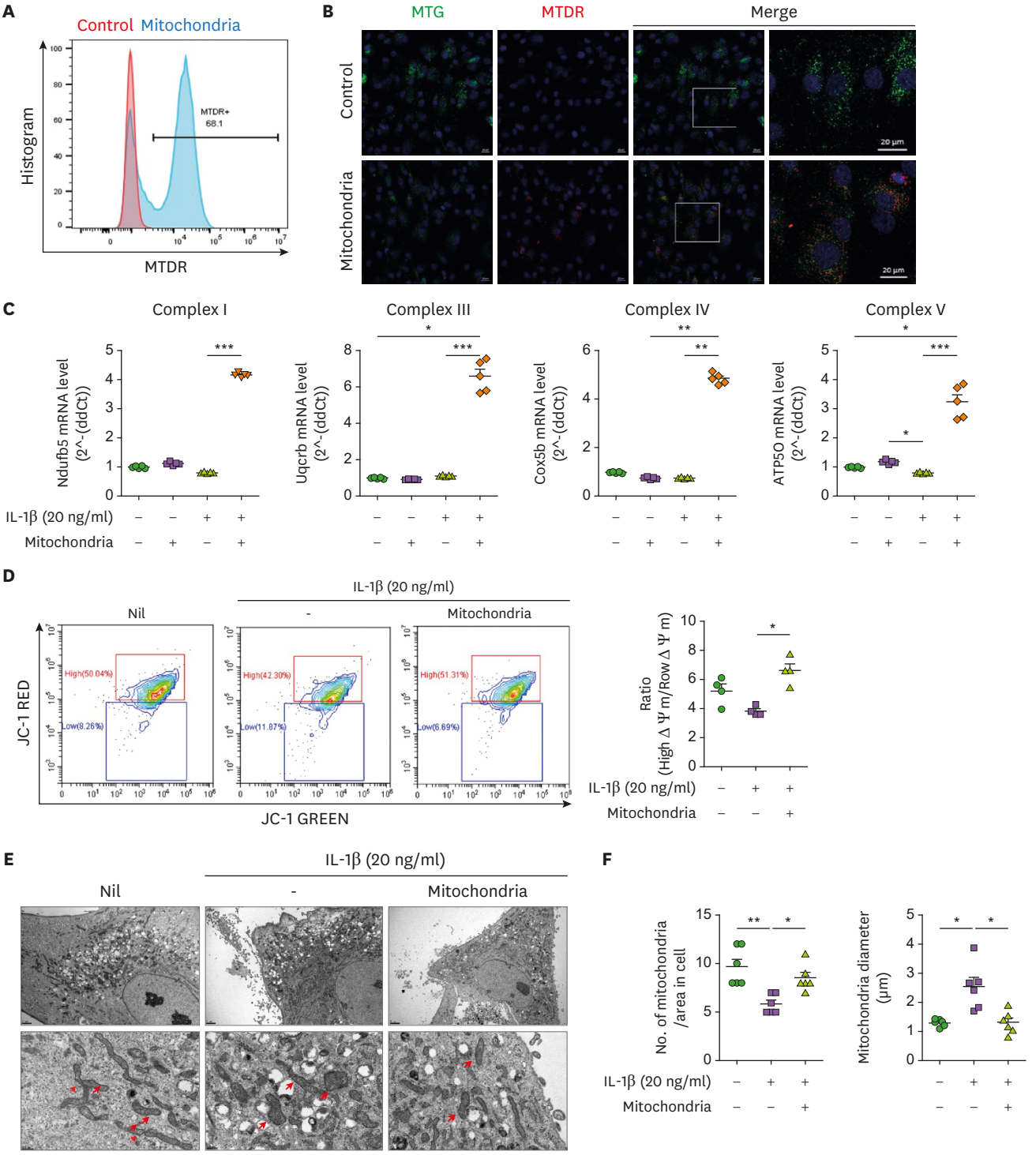

Figure 3. Improvement of mitochondrial function in human OA chondrocytes by mitochondrial transplantation. MTDR-stained mitochondria were transferred into human chondrocytes with MTG-labeled mitochondria. (A) Representative FACS plot shows percentages of MTDR-positive cells. (B) Representative images show MTG (greed), MTDR (red), and DAPI (blue) positive cells. Scale bar = 20 μm. (C) mtOXPHOS Complex genes were determined by RT-qPCR in OA chondrocytes incubated in the presence or absence of IL-1β (20 ng/mL) and mitochondria (5 μg) for 24 h. Average transcript levels of complex I, III, IV, and V. (D) Mitochondrial membrane potential analyzed by JC-1 staining. (E) Transmission electron micrographs of chondrocytes from OA patients in the presence or absence of IL-1β (20 ng/mL) and mitochondria (5 μg) for 24 h. Arrowheads, mitochondria. Scale: 2 μm (upper panels), 0.5 μm (lower panels). (F) The average number of mitochondria (left) and mitochondrial diameter (right). Data are means ± SEM.
*p<0.05, **p<0.01, ***p<0.001.

https://doi.org/10.4110/in.2022.22.e14

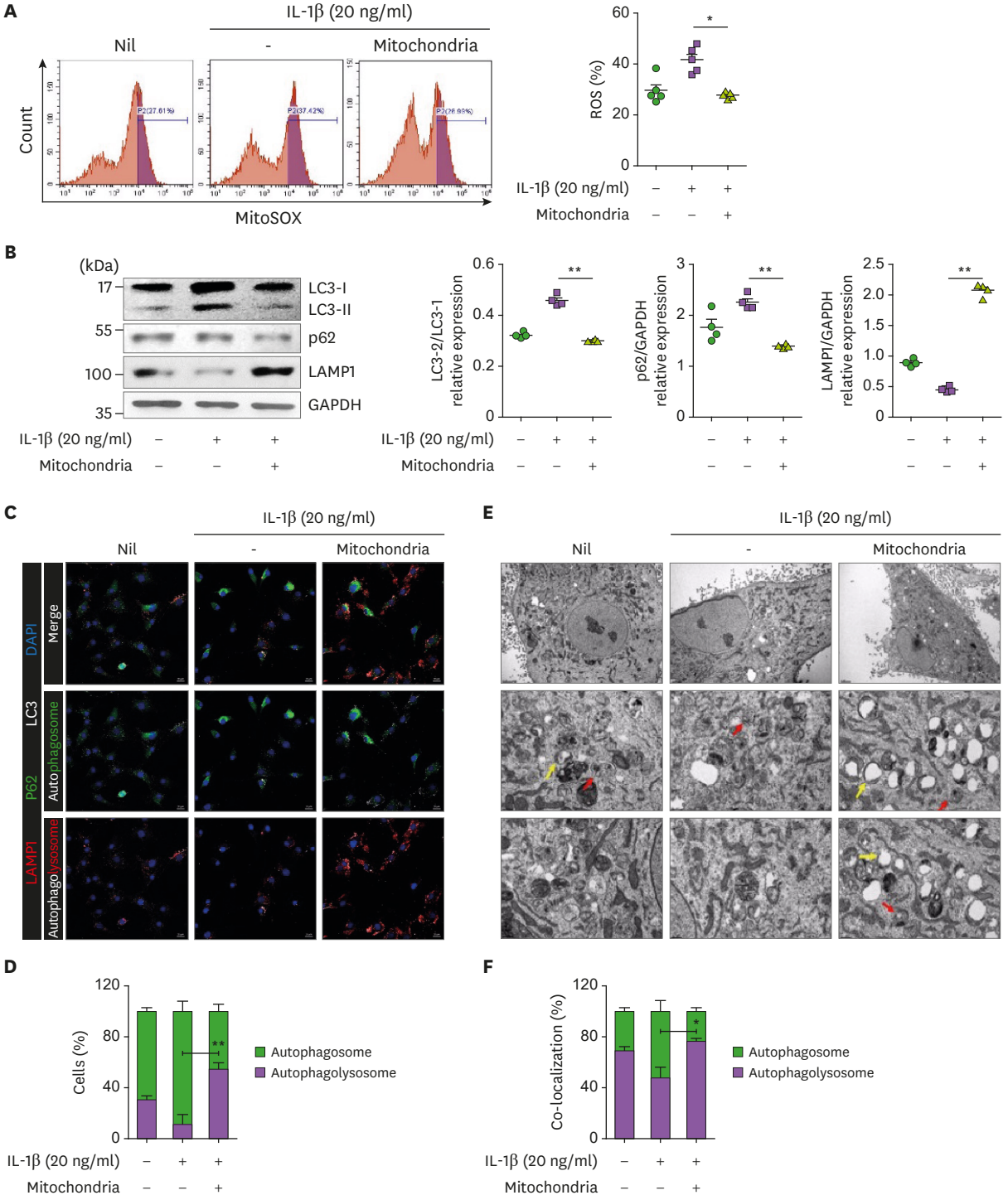

Figure 4. Regulation of autophagy activity by mitochondrial transfer. Human OA chondrocytes were cultured with mitochondria (5 μg) in the presence or absence of IL-1β (20 ng/mL) for 24 h. (A) Mitochondrial ROS was measured using MitoSOX dye and flow cytometry. Bar graph shows averaged amount of ROS in each condition. (B) Representative immunoblots show LC3, p62, and LAMP1 in each condition. Average LC-3I and LC-3II (left), p62 and GAPDH (middle), and LAMP1 and GAPDH (right) ratio. (C) Confocal micrographs show colocalization of p62 (FITC) and LC3 (APC), and LAMP1 (PE) and LC3 (APC) for autophagosome and autophagolysosome, respectively. Scale bar = 20 μm. (D) Percentages of cells with autophagosomes and autophagolysosomes. (E) Autophagy was analyzed by TEM. Red arrows, autophagosomes; yellow arrows, autophagolysosomes. Scale bar = 2 μm (upper panels), 0.5 μm (lower panels). (F) Percentages of cells with autophagosomes and autophagolysosomes. Data are means ± SEM.
*p<0.05, **p<0.01.

https://doi.org/10.4110/in.2022.22.e14

Mitochondrial transfer reduced catabolic and inflammatory cell death markers

The catabolic factors MMP-1, MMP-3, and MMP-13 were decreased by mitochondrial transplantation (**Fig. 5A**). Necrosis of OA chondrocytes was increased by IL-1β and improved by mitochondrial transplantation (**Fig. 5B**). Also, the expression of the inflammatory cell death markers, phospho- or total of RIPK1, RIPK3, and MLKL, was increased by IL-1β or TNF-α, and it was recovered by mitochondrial transplantation (**Fig. 5C**). The mRNA levels of col2a1 and aggrecan, which are components of cartilage, were increased by mitochondrial transplantation (**Fig. 5D**).

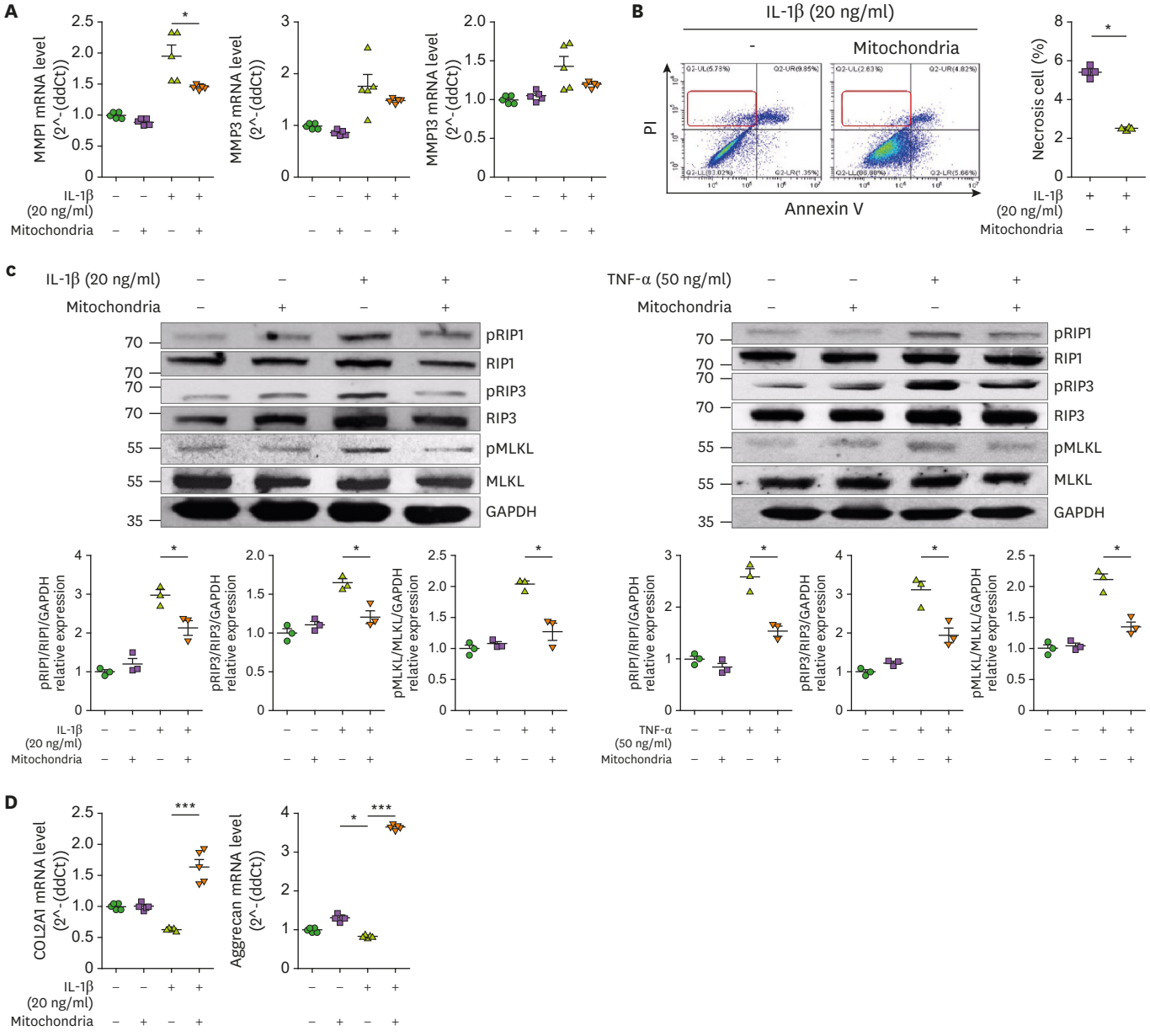

Figure 5. Expression of cell death and cartilage regulatory markers following mitochondria administration. Human OA chondrocytes were cultured in the presence or absence of IL-1β (20 ng/mL) or TNF-α (50 ng/ml) and mitochondria (5 μg) for 24 h. (A) mRNA levels of catabolic factors were analyzed by qPCR. (B) Necrosis analysis by annexinV/PI staining. (C) Expression of phospho- or total of RIPK1, RIPK3, MLKL in OA chondrocytes was analyzed by western blotting. (D) mRNA levels of chondrogenesis markers in OA chondrocytes. Data are means ± SEM.
*p<0.05, ***p<0.001.

https://doi.org/10.4110/in.2022.22.e14

Effect of xenogeneic mitochondrial transplantation on MIA-induced OA

The PWL, PWT, and weight-bearing were significantly improved in the mitochondria-transplantation group compared with the control group (**Fig. 6A and B**). Histopathological and micro-CT data showed the therapeutic effect of mitochondrial transplantation in cartilage destruction and bone loss in the knee joint (**Fig. 6C and D**). Also, the expression of IL-1β, TNF-α, MMP-13, and pMLKL was decreased in the mitochondria-transplantation group (**Fig. 6E**).

DISCUSSION

This is the first report of a protective effect of exogenous mitochondrial transplantation on OA. We aimed to ameliorate OA development and progression by mitochondrial transplantation *in vivo* and *in vitro*. We obtained mitochondria from L6 cells and administered them to OA animals as well as OA chondrocytes. We evaluated OA progression and expression of OA-related factors.

MMP-induced cartilage destruction is a hallmark of OA (30-32). MMP-13 targets cartilage for degradation and its expression level is affected by IL-1β and TNF-α (33,34). The MCP-1-CCR2 axis plays a crucial role in the development and progression of OA (35,36). Phosphorylation of MLKL by the protein kinase RIPK3 induces necroptosis (37,38) and OA progression (39,40). Clinical phenotypes such as pain management, cartilage destruction, and bone resorption were in support of mitochondrial transplantation. Also, mitochondrial transplantation decreases the levels of IL-1β, TNF-α, MCP-1, MMP-13, and pMLKL.

Mitochondrial dysfunction occurs during OA progression (9,10) and manifests as decreased ATP synthesis, decreased membrane potential, and increased oxidative stress, resulting in cartilage destruction (41). Mitochondrial dysfunction induces IL-1b release and leads to inflammation in chondrocytes by decreasing respiratory chain complex activity (7,42). Mitochondrial morphology and structure are impaired in OA chondrocytes (9,16). Mitochondria are swollen and mitochondrial cristae are decreased in OA chondrocytes. In this study, the impaired mitochondrial morphology decreased mitochondrial membrane potential, and expression of respiratory chain complexes was improved in mitochondrial transferred chondrocytes. Therefore, mitochondrial transplantation ameliorates OA progression by improving mitochondrial function.

Autophagy is the self-degradative cellular and molecular mechanism that removes dysfunctional or unnecessary proteins and organelles (43). There are three types of autophagy: macro-autophagy, micro-autophagy, and chaperone-mediated autophagy, which promote proteolytic degradation by the lysosome (44). Impaired autophagy is related to disease development and progression (45,46). Autophagy is impaired in OA animal models (47) and OA patients (48). ROS is essential for autophagy and regulates the activity of ATG4, a protease critical for autophagy (49). Increased ROS inhibits ATG4 activity, suppressing autophagic influx. There is a relationship between autophagy and apoptosis, however, little is known of the relationship between autophagy and necroptosis. In this study, necroptosis was decreased, and impaired autophagy was improved by mitochondrial transplantation by regulating ROS activity.

Mitochondrial transplantation, even of autologous mitochondria, can induce an immune response (50). By contrast, another group found no inflammation after mitochondrial

https://doi.org/10.4110/in.2022.22.e14

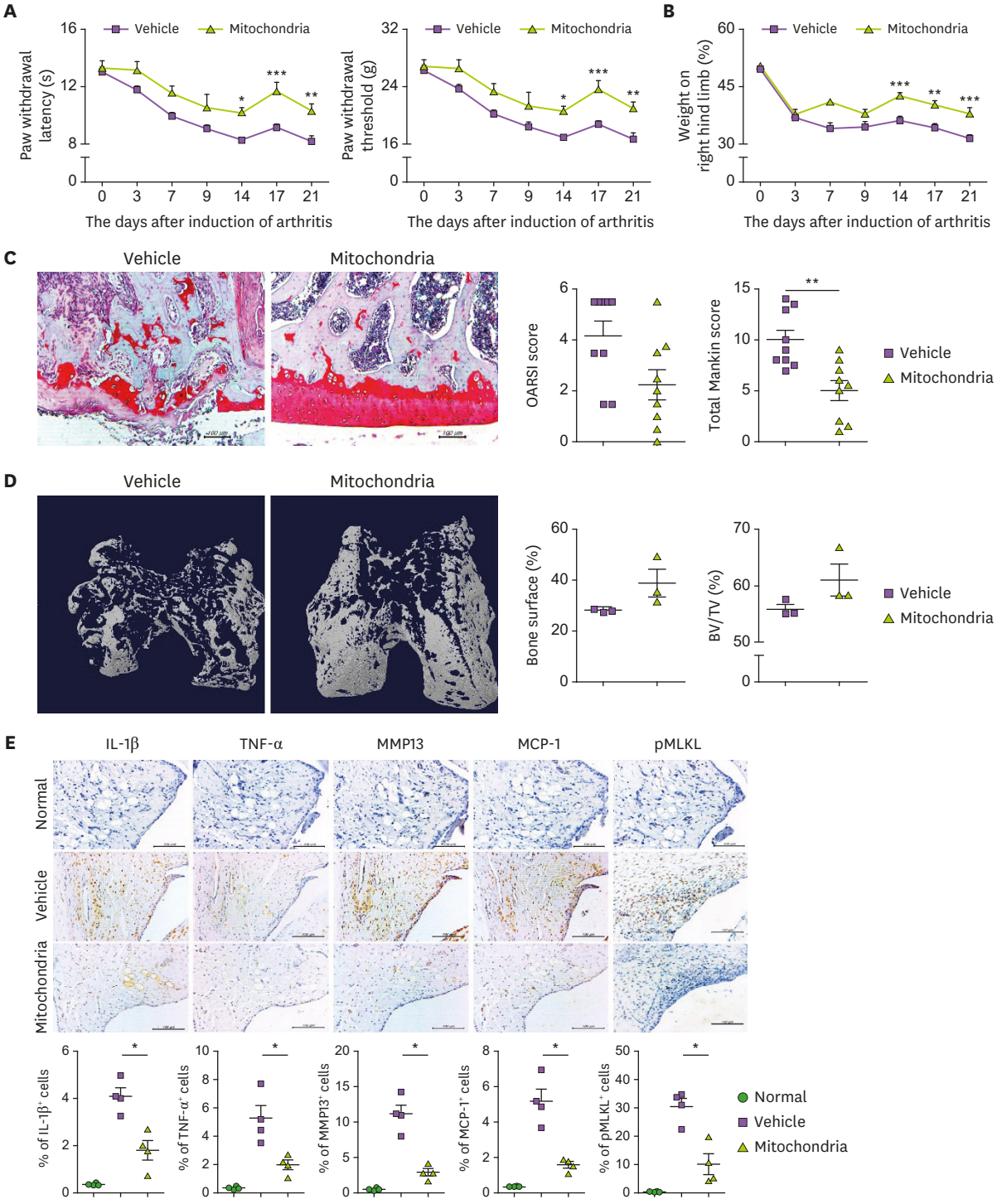

Figure 6. Mitochondrial transplantation from OA patient muscle tissue in MIA-induced rat joint. MIA-induced OA rats were evaluated for 21 days (n=3 animals per group). Intra-articular mitochondria injection was performed twice weekly. Kinetics of PWL, PWT (A), and weight-bearing (B). (C) Representative images show Safranin O-stained cartilage. Bar graphs show averaged total Mankin score (left) and OARIS score (right). (D) Representative micro-CT images show bone of each group. Bar graphs show percentage of bone surface (left) and BV: TV ratio (right). (E) IL-1β, TNF-α, MCP-1, MMP-13, and pMLKL expression determined immunohistochemically in the synovium of MIA-induced OA rats. Data are means ± SEM.
*p<0.05, **p<0.01.

https://doi.org/10.4110/in.2022.22.e14

transplantation (51). In this study, there was no inflammation or allogeneic or xenogeneic transplantation. Also, there was no immune response after mitochondrial transplantation, but this needs to be verified by further studies.

The development of OA is accelerated by joint deformity and instability. Intraarticular ligaments promote static stability of joints and muscles and tendons around joints provide dynamic stability. Therefore, mitochondrial transplantation to muscle and tendon around joints can strengthen muscle and protect joints from OA.

Mitochondrial transplantation was first applied for ischemic disease. Mitochondrial transplantation protects and promotes the regeneration of chondrocytes. Also, compared to cellular therapeutics, mitochondrial transplantation maintains cellular homeostasis and regulates inflammation and cell death. In this study, we demonstrate the therapeutic potential of mitochondrial transplantation for OA. OA development and progression were ameliorated by mitochondrial transplantation by regulating inflammatory and catabolic factors. Mitochondrial transplantation improved mitochondrial dysfunction and activated autophagy by inhibiting ROS activity. Mitochondrial transplantation ameliorated OA progression, which is caused by mitochondrial dysfunction. Our findings indicate the therapeutic potential of mitochondrial transplantation for OA.

ACKNOWLEDGEMENTS

This research was supported by a grant of the Korea Health Technology R&D Project through the Korea Health Industry Development Institute (KHIDI), funded by the Ministry of Health & Welfare, Republic of Korea (grant number HI20C1496).

SUPPLEMENTARY MATERIALS

Supplementary Table 1

List of primers for real-time PCR in this study

Click here to view

Supplementary Figure 1

Mitochondrial transplantation suppressed inflammatory mediators in the MIA-induced model. OA rats were sacrificed at day 29 after induction and joint tissues were stained with indicated antibodies (n=5 animals per group). (A) The expression of pro-inflammatory cytokines (IL-1β, TNF-α), MCP-1, catabolic factor (MMP-13), and necroptosis marker (p-MLKL) was determined immunohistochemically in the synovium of MIA-induced OA rats. (B) Bar graphs show the percentage of positive cells for each antibody. The data are expressed as the mean±SEM ($^{*}p<0.05$).

Click here to view

Supplementary Figure 2

Mitochondrial transplantation ameliorates the development and progression of osteoarthritis.

Click here to view

REFERENCES

1. Martel-Pelletier J, Barr AJ, Cicuttini FM, Conaghan PG, Cooper C, Goldring MB, Goldring SR, Jones G, Teichtahl AJ, Pelletier JP. Osteoarthritis. *Nat Rev Dis Primers* 2016;2:16072.
PUBMED | CROSSREF
2. Hunter DJ, Bierma-Zeinstra S. Osteoarthritis. *Lancet* 2019;393:1745-1759.
PUBMED | CROSSREF
3. Habiballa L, Salmonowicz H, Passos JF. Mitochondria and cellular senescence: Implications for musculoskeletal ageing. *Free Radic Biol Med* 2019;132:3-10.
PUBMED | CROSSREF
4. Palazzo C, Nguyen C, Lefevre-Colau MM, Rannou F, Poiraudeau S. Risk factors and burden of osteoarthritis. *Ann Phys Rehabil Med* 2016;59:134-138.
PUBMED | CROSSREF
5. Zhou B, Tian R. Mitochondrial dysfunction in pathophysiology of heart failure. *J Clin Invest* 2018;128:3716-3726.
PUBMED | CROSSREF
6. Jin HS, Suh HW, Kim SJ, Jo EK. Mitochondrial control of innate immunity and inflammation. *Immune Netw* 2017;17:77-88.
PUBMED | CROSSREF
7. Blanco FJ, Rego I, Ruiz-Romero C. The role of mitochondria in osteoarthritis. *Nat Rev Rheumatol* 2011;7:161-169.
PUBMED | CROSSREF
8. Phull AR, Eo SH, Abbas Q, Ahmed M, Kim SJ. Applications of chondrocyte-based cartilage engineering: an overview. *BioMed Res Int* 2016;2016:1879837.
PUBMED | CROSSREF
9. Liu H, Li Z, Cao Y, Cui Y, Yang X, Meng Z, Wang R. Effect of chondrocyte mitochondrial dysfunction on cartilage degeneration: a possible pathway for osteoarthritis pathology at the subcellular level. *Mol Med Rep* 2019;20:3308-3316.
PUBMED | CROSSREF
10. Ansari MY, Ahmad N, Voleti S, Wase SJ, Novak K, Haqqi TM. Mitochondrial dysfunction triggers a catabolic response in chondrocytes via ROS-mediated activation of the JNK/AP1 pathway. *J Cell Sci* 2020;133:jcs247353.
PUBMED | CROSSREF
11. Sun K, Jing X, Guo J, Yao X, Guo F. Mitophagy in degenerative joint diseases. *Autophagy* 2021;17:2082-2092.
PUBMED | CROSSREF
12. Blanco FJ, López-Armada MJ, Maneiro E. Mitochondrial dysfunction in osteoarthritis. *Mitochondrion* 2004;4:715-728.
PUBMED | CROSSREF
13. Gavriilidis C, Miwa S, von Zglinicki T, Taylor RW, Young DA. Mitochondrial dysfunction in osteoarthritis is associated with down-regulation of superoxide dismutase 2. *Arthritis Rheum* 2013;65:378-387.
PUBMED | CROSSREF
14. Kim H, Kang D, Cho Y, Kim JH. Epigenetic regulation of chondrocyte catabolism and anabolism in osteoarthritis. *Mol Cells* 2015;38:677-684.
PUBMED | CROSSREF
15. Mueller MB, Tuan RS. Anabolic/catabolic balance in pathogenesis of osteoarthritis: identifying molecular targets. *PM R* 2011;3:S3-S11.
PUBMED | CROSSREF
16. Liu JT, Guo X, Ma WJ, Zhang YG, Xu P, Yao JF, Bai YD. Mitochondrial function is altered in articular chondrocytes of an endemic osteoarthritis, Kashin-Beck disease. *Osteoarthritis Cartilage* 2010;18:1218-1226.
PUBMED | CROSSREF
17. Coleman MC, Goetz JE, Brouillette MJ, Seol D, Willey MC, Petersen EB, Anderson HD, Hendrickson NR, Compton J, Khorsand B, et al. Targeting mitochondrial responses to intra-articular fracture to prevent posttraumatic osteoarthritis. *Sci Transl Med* 2018;10:eaan5372.
PUBMED | CROSSREF
18. Jung HE, Shim YR, Oh JE, Oh DS, Lee HK. The autophagy protein atg5 plays a crucial role in the maintenance and reconstitution ability of hematopoietic stem cells. *Immune Netw* 2019;19:e12.
PUBMED | CROSSREF
19. Ansari MY, Ball HC, Wase SJ, Novak K, Haqqi TM. Lysosomal dysfunction in osteoarthritis and aged cartilage triggers apoptosis in chondrocytes through BAX mediated release of cytochrome c. *Osteoarthritis Cartilage* 2021;29:100-112.
PUBMED | CROSSREF

20. Na HS, Kwon JY, Lee SY, Lee SH, Lee AR, Woo JS, Jung K, Cho KH, Choi JW, Lee DH, et al. Metformin attenuates monosodium-iodoacetate-induced osteoarthritis via regulation of pain mediators and the autophagy-lysosomal pathway. *Cells* 2021;10:681.
PUBMED | CROSSREF

21. Weixler V, Lapusca R, Grangl G, Guariento A, Saeed MY, Cowan DB, Del Nido PJ, McCully JD, Friehs I. Autogenous mitochondria transplantation for treatment of right heart failure. *J Thorac Cardiovasc Surg* 2021;162:e111-e121.
PUBMED | CROSSREF

22. Doulamis IP, Guariento A, Duignan T, Kido T, Orfany A, Saeed MY, Weixler VH, Blitzer D, Shin B, Snay ER, et al. Mitochondrial transplantation by intra-arterial injection for acute kidney injury. *Am J Physiol Renal Physiol* 2020;319:F403-F413.
PUBMED | CROSSREF

23. Chang JC, Chang HS, Wu YC, Cheng WL, Lin TT, Chang HJ, Kuo SJ, Chen ST, Liu CS. Mitochondrial transplantation regulates antitumour activity, chemoresistance and mitochondrial dynamics in breast cancer. *J Exp Clin Cancer Res* 2019;38:30.
PUBMED | CROSSREF

24. Espino De la Fuente-Muñoz C, Arias C. The therapeutic potential of mitochondrial transplantation for the treatment of neurodegenerative disorders. *Rev Neurosci* 2020;32:203-217.
PUBMED | CROSSREF

25. Zhao Z, Hou Y, Zhou W, Keerthiga R, Fu A. Mitochondrial transplantation therapy inhibit carbon tetrachloride-induced liver injury through scavenging free radicals and protecting hepatocytes. *Bioeng Transl Med* 2020;6:e10209.
PUBMED

26. Hwang JW, Lee MJ, Chung TN, Lee HAR, Lee JH, Choi SY, Park YJ, Kim CH, Jin I, Kim SH, et al. The immune modulatory effects of mitochondrial transplantation on cecal slurry model in rat. *Crit Care* 2021;25:20.
PUBMED | CROSSREF

27. Boutagy NE, Pyne E, Rogers GW, Ali M, Hulver MW, Frisard MI. Isolation of mitochondria from minimal quantities of mouse skeletal muscle for high throughput microplate respiratory measurements. *J Vis Exp* 2015;105:53217.
PUBMED | CROSSREF

28. Pritzker KP, Gay S, Jimenez SA, Ostergaard K, Pelletier JP, Revell PA, Salter D, van den Berg WB. Osteoarthritis cartilage histopathology: grading and staging. *Osteoarthritis Cartilage* 2006;14:13-29.
PUBMED | CROSSREF

29. Kim EK, Kwon JE, Lee SY, Lee EJ, Kim DS, Moon SJ, Lee J, Kwok SK, Park SH, Cho ML. IL-17-mediated mitochondrial dysfunction impairs apoptosis in rheumatoid arthritis synovial fibroblasts through activation of autophagy. *Cell Death Dis* 2017;8:e2565.
PUBMED | CROSSREF

30. Blom AB, van Lent PL, Libregts S, Holthuysen AE, van der Kraan PM, van Rooijen N, van den Berg WB. Crucial role of macrophages in matrix metalloproteinase-mediated cartilage destruction during experimental osteoarthritis: involvement of matrix metalloproteinase 3. *Arthritis Rheum* 2007;56:147-157.
PUBMED | CROSSREF

31. Goldring MB, Otero M, Plumb DA, Dragomir C, Favero M, El Hachem K, Hashimoto K, Roach HI, Olivotto E, Borzì RM, et al. Roles of inflammatory and anabolic cytokines in cartilage metabolism: signals and multiple effectors converge upon MMP-13 regulation in osteoarthritis. *Eur Cell Mater* 2011;21:202-220.
PUBMED | CROSSREF

32. Inada M, Wang Y, Byrne MH, Rahman MU, Miyaura C, López-Otín C, Krane SM. Critical roles for collagenase-3 (Mmp13) in development of growth plate cartilage and in endochondral ossification. *Proc Natl Acad Sci U S A* 2004;101:17192-17197.
PUBMED | CROSSREF

33. Sutton CE, Lalor SJ, Sweeney CM, Brereton CF, Lavelle EC, Mills KH. Interleukin-1 and IL-23 induce innate IL-17 production from gammadelta T cells, amplifying Th17 responses and autoimmunity. *Immunity* 2009;31:331-341.
PUBMED | CROSSREF

34. Scanzello CR, Umoh E, Pessler F, Diaz-Torne C, Miles T, Dicarlo E, Potter HG, Mandl L, Marx R, Rodeo S, et al. Local cytokine profiles in knee osteoarthritis: elevated synovial fluid interleukin-15 differentiates early from end-stage disease. *Osteoarthritis Cartilage* 2009;17:1040-1048.
PUBMED | CROSSREF

35. Miller RE, Tran PB, Das R, Ghoreishi-Haack N, Ren D, Miller RJ, Malfait AM. CCR2 chemokine receptor signaling mediates pain in experimental osteoarthritis. *Proc Natl Acad Sci U S A* 2012;109:20602-20607.
PUBMED | CROSSREF

36. Xu YK, Ke Y, Wang B, Lin JH. The role of MCP-1-CCR2 ligand-receptor axis in chondrocyte degradation and disease progress in knee osteoarthritis. *Biol Res* 2015;48:64.
PUBMED | CROSSREF

37. Samson AL, Zhang Y, Geoghegan ND, Gavin XJ, Davies KA, Mlodzianoski MJ, Whitehead LW, Frank D, Garnish SE, Fitzgibbon C, et al. MLKL trafficking and accumulation at the plasma membrane control the kinetics and threshold for necroptosis. *Nat Commun* 2020;11:3151.
PUBMED | CROSSREF

38. Yoon S, Kovalenko A, Bogdanov K, Wallach D. MLKL, the protein that mediates necroptosis, also regulates endosomal trafficking and extracellular vesicle generation. *Immunity* 2017;47:51-65.e7.
PUBMED | CROSSREF

39. Liang S, Wang ZG, Zhang ZZ, Chen K, Lv ZT, Wang YT, Cheng P, Sun K, Yang Q, Chen AM. Decreased RIPK1 expression in chondrocytes alleviates osteoarthritis via the TRIF/MyD88-RIPK1-TRAF2 negative feedback loop. *Aging (Albany NY)* 2019;11:8664-8680.
PUBMED | CROSSREF

40. Shan B, Pan H, Najafov A, Yuan J. Necroptosis in development and diseases. *Genes Dev* 2018;32:327-340.
PUBMED | CROSSREF

41. Cheleschi S, Cantarini L, Pascarelli NA, Collodel G, Lucherini OM, Galeazzi M, Fioravanti A. Possible chondroprotective effect of canakinumab: an *in vitro* study on human osteoarthritic chondrocytes. *Cytokine* 2015;71:165-172.
PUBMED | CROSSREF

42. Wang Y, Zhao X, Lotz M, Terkeltaub R, Liu-Bryan R. Mitochondrial biogenesis is impaired in osteoarthritis chondrocytes but reversible via peroxisome proliferator-activated receptor γ coactivator 1α. *Arthritis Rheumatol* 2015;67:2141-2153.
PUBMED | CROSSREF

43. Klionsky DJ. Autophagy revisited: a conversation with Christian de Duve. *Autophagy* 2008;4:740-743.
PUBMED | CROSSREF

44. Glick D, Barth S, Macleod KF. Autophagy: cellular and molecular mechanisms. *J Pathol* 2010;221:3-12.
PUBMED | CROSSREF

45. Yin H, Wu H, Chen Y, Zhang J, Zheng M, Chen G, Li L, Lu Q. The therapeutic and pathogenic role of autophagy in autoimmune diseases. *Front Immunol* 2018;9:1512.
PUBMED | CROSSREF

46. Hsu HC, Chen YH, Lin TS, Shen CY, Hsieh SC. Systemic lupus erythematosus is associated with impaired autophagic degradation via interleukin-6 in macrophages. *Biochim Biophys Acta Mol Basis Dis* 2021;1867:166027.
PUBMED | CROSSREF

47. Zhou H, Li G, Wang Y, Jiang R, Li Y, Wang H, Wang F, Ma H, Cao L. Microbial metabolite sodium butyrate attenuates cartilage degradation by restoring impaired autophagy and autophagic flux in osteoarthritis development. *Front Pharmacol* 2021;12:659597.
PUBMED | CROSSREF

48. Feng L, Feng C, Wang CX, Xu DY, Chen JJ, Huang JF, Tan PL, Shen JM. Circulating microRNA let-7e is decreased in knee osteoarthritis, accompanied by elevated apoptosis and reduced autophagy. *Int J Mol Med* 2020;45:1464-1476.
PUBMED | CROSSREF

49. Scherz-Shouval R, Shvets E, Fass E, Shorer H, Gil L, Elazar Z. Reactive oxygen species are essential for autophagy and specifically regulate the activity of Atg4. *EMBO J* 2007;26:1749-1760.
PUBMED | CROSSREF

50. Kesner EE, Saada-Reich A, Lorberboum-Galski H. Characteristics of mitochondrial transformation into human cells. *Sci Rep* 2016;6:26057.
PUBMED | CROSSREF

51. Kitani T, Kami D, Matoba S, Gojo S. Internalization of isolated functional mitochondria: involvement of macropinocytosis. *J Cell Mol Med* 2014;18:1694-1703.
PUBMED | CROSSREF